Optical Phonons in Mixed Crystals of $CdSe_ySe_{1-y}$

H. W. VERLEUR* AND A. S. BARKER, JR.
Bell Telephone Laboratories, Murray Hill, New Jersey
(Received 23 September 1966)

The infrared reflectivity spectra of mixed crystals of $CdSe_ySe_{1-y}$ have been measured at 15 and 300°K. The infrared-active phonons occur in two main bands with frequencies near those of pure CdS and pure CdSe. Some features of the spectra are similar to the lattice vibrations in the $GaAs_yP_{1-y}$ system. The model used for that system is extended to the wurtzite structure. The main features of this model are the dependence of the phonon frequencies and strengths on concentration y and on the short-range clustering of the cations around the anions. Compared with $GaAs_yP_{1-y}$, the clustering behavior is found to be significantly less for the present system.

INTRODUCTION

IN a previous paper,[1] henceforth to be referred to as I, the far-infrared reflectivity spectrum of the alloy $GaAs_yP_{1-y}$ was studied for various values of y between 0 and 1. A harmonic model was developed for the optical-lattice vibrations of the alloy from which the infrared reflectivity was calculated as a function of frequency and composition (y), and a short-range clustering parameter β. The theoretical reflectivity curves were in good agreement with the experimentally measured ones at all compositions studied.

The basic model used to describe $GaAs_yP_{1-y}$ is relatively general, and should apply to other alloy systems of the type XY_yZ_{1-y}, especially those in which short-range forces strongly influence the lattice dynamics. To test the model further, we have studied the far-infrared reflectivity spectra of $CdSe_ySe_{1-y}$ crystals at 300 and at 15°K. The results, described in this paper, confirm that the model also applies to this new system, and suggest significantly different degrees of short-range clustering for the $GaAs_yP_{1-y}$ and $CdSe_ySe_{1-y}$ systems.

Mixed crystals of $CdSe_ySe_{1-y}$ can be grown as single crystals over the whole composition range $y=0$ to 1. They are known to crystallize in the wurtzite structure as do the parent crystals CdS and CdSe. In CdS and CdSe, the primitive unit cell contains four ions. In the alloys, however, the irregular distribution of the Se and S ions over the negative-ion sublattice does not allow us to define such a primitive unit cell. As was done in I, we avoid this difficulty by concentrating on the various possible nearest-neighbor arrangements of anions around the cations. As before, we weight the different configurations statistically, and include the possibility of clustering. Although we will also be concerned with second-neighbor interactions, our basic assumptions are that nearest-neighbor interactions dominate, and that an average Se-S distribution is sufficient for the description of second-neighbor interactions.

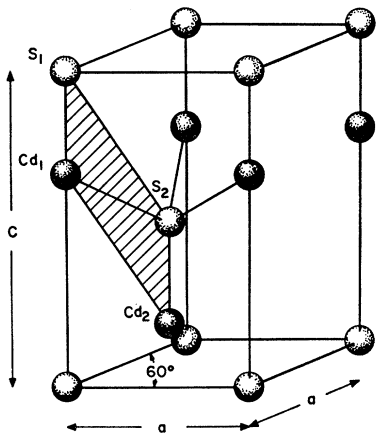

FIG. 1. Unit cell of the wurtzite structure, showing nearest-neighbor unit of four negative ions forming a tetrahedron with positive ion at the center.

In preparation for the more complex cases that follow, we discuss in the following section a detailed harmonic model with one active optic mode which is suitable for the pure crystals CdS and CdSe, and which illustrates how the basic model of Paper I must be generalized to include optical anisotropy and the effective field. These effects cause some differences between the zinc-blende structure of I and the wurtzite structure considered here.

In the third section, we describe the experimental reflectivity spectra, and compare our results with those of other investigators. At 300°K, the reflectivity spectrum of CdS exhibits structure due to anharmonicity which is either absent or strongly suppressed at 15°K. To simplify interpretation, we compare our harmonic model only with the low-temperature measurements. We will then find that with a minor modification, the model developed in Paper I accounts quantitatively for the significant features of the reflectivity spectra of $CdSe_ySe_{1-y}$ at all values of y considered.

Brodsky and Burstein's suggestion[2] that the effective ionic charge in II–VI compounds has a local and nonlocal portion is supported by the results obtained in this work. Values for these two effective charges of CdS and CdSe are obtained as best-fit parameters to the experimental reflectivity curves. Finally, we will find that a substantial improvement in the theoretical fit of the

* Work performed in partial fulfillment of the requirements for the Ph.D. degree, New York University.

[1] H. W. Verleur and A. S. Barker, Jr., Phys. Rev. 149, 715 (1966).

[2] M. Brodsky and E. Burstein, Bull. Am. Phys. Soc. 7, 214 (1962). See also E. Burstein, in *Phonons and Phonon Interactions*, edited by Thor. A. Bak (W. A. Benjamin, Inc., New York, 1964), p. 276.

experimental reflectivity curves is obtained if it is assumed that the presence of sulphur in the mixed crystals causes an increase in the ionicity of the Cd-Se bond.

OPTICAL-PHONON VIBRATIONS IN THE WURTZITE STRUCTURE

A. The Equation of Motion

The unit cell of CdS (or CdSe) is shown in Fig. 1. It contains two formula units (i.e., four ions). Group theory shows that the phonon-dispersion curves consist of three acoustic branches and nine optic branches. At very small wave vector ($\mathbf{q}=0$), three of the latter are infrared-active modes of vibration (one doubly degenerate E_1 type and one A_1 type). The remaining six optic modes are normally infrared-inactive. We shall not be concerned with these inactive modes. In Fig. 2(a), we have shown schematically the ion motions of the fundamental infrared-active modes of vibration for the wave vector chosen in the y direction.

For certain directions of $\mathbf{q}$, the E_1-type modes have their degeneracy removed by the macroscopic polarization field. In Fig. 2(b), all the infrared dispersion curves are shown, and the polarization directions labeled. It should be noted that the figures are drawn for $\mathbf{q}$ much smaller than the size of the first Brillouin zone, but larger than about 4×10^3 cm^{-1}, i.e., outside the polariton region. This is the region usually signified by $\mathbf{q}\approx0$. As can be seen from the figure, there are four distinct optical frequencies at $\mathbf{q}\approx0$. For light polarized along the z axis (or c axis) the A_1 transverse-optic (TO) and longitudinal-optic (LO) modes are detected. For light polarized perpendicular to the c axis, the E_1 TO and LO modes are detected.

Although we have four ions per unit cell, in the wurtzite structure the two negative ions (or the two positive ions) have identical, though rotated, surroundings. Moreover, in the infrared-active modes (at $\mathbf{q}\approx0$), the Cd ions are not relatively displaced. Neither are the Se (or S) ions. Therefore, for the purpose of calculating the strengths and frequencies of these modes, we will not distinguish between the two positive or between the two negative ions. Effectively then, we consider a unit cell containing only two ions.

For the positive and negative ions vibrating relative to one another in a fundamental TO mode under the influence of an electromagnetic field, we write the following equation of motion and expression for the dielectric polarization:

$$\ddot{u}(i)=\frac{-k(i)}{\bar{m}}u(i)+\frac{e(i)}{\bar{m}}E_{\text{eff}}(i), \tag{1}$$

and

$$P(i)=Ne(i)u(i)+N(\alpha_+ +\alpha_-)E_{\text{eff}}(i), \tag{2}$$

where $u(i)=w_+(i)-w_-(i)$ is the relative displacement of the positive and negative ions along the ith direction. This direction is chosen either perpendicular or parallel to the c axis. $\bar{m}=m_+m_-/(m_++m_-)$ is the effective ionic mass. These equations (without, however, the direction dependence expressed by i) were generalized in I for mixed crystals of $GaAs_yP_{1-y}$ with several sublattices. We use Eqs. (1) and (2) here to illustrate several points connected with the lattice dynamics. $k(i)$ is the short-range force constant representing the interaction of 1st, 3rd, etc. neighbors. 2nd, 4th, etc. neighbors are not relatively displaced in these modes. Since the distribution of 3rd, 5th, etc. neighbors is not isotropic, we use different values for the $k(i)$ depending on whether the vibration direction is chosen perpendicular or parallel to the c axis. Similarly, $e(i)$, the effective ionic charge, requires two values for the two principal directions of vibration. In Eq. (2), the first term represents the ionic polarization arising from the atomic displacements, where N is the number of ion pairs per unit volume, i.e., we work with the smaller cell described above which is appropriate to the infrared modes. The second term in Eq. (2) is the electronic polarization of the atoms induced by the effective local field E_{eff}, where α_+ and α_- are the polarizabilities of the positive and negative ions.

B. The Effective Field

For the situation in which all charges are assumed to be completely localized, the effective field on an ion

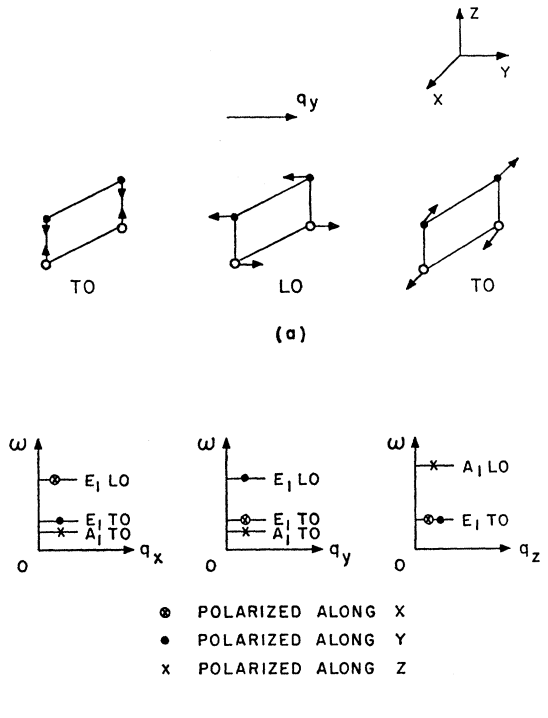

FIG. 2. (a) Infrared-active normal modes of vibration of primitive unit cell in wurtzite, with wave propagating along y direction. (b) Phonon dispersion curves near $\mathbf{q}=0$.

E_{eff} for a $\mathbf{q}\approx 0$ transverse wave is

$$\mathbf{E}_{\text{eff}}=\mathbf{E}+\frac{4\pi\mathbf{P}}{3}+\sum_{\text{sphere}}\mathbf{E}_d, \tag{3}$$

where $\mathbf{E}$ is the macroscopic field, $4\pi\mathbf{P}/3$ is the contribution to the field from the surface polarization of the Lorentz sphere centered on that ion, and the last term is the field due to all point dipoles within that sphere. When the lattice has cubic symmetry, this last term vanishes for all modes of vibration.[3] In the case of CdS and CdSe, however, the last term is finite, and the contribution to the effective field from the dipoles depends on the vibrational modes, and the vibration direction considered. Methods for calculating this third term have been suggested by Slater, Kornfeld, and others, and are summarized by Kittel.[4] We have carried out the calculation of $\mathbf{E}_{\text{eff}}$ for the ideal wurtzite structure. Labeling the four sites in the unit cell of CdS as Cd_1, Cd_2, S_1, and S_2 (Fig. 1), then the effective field at the Cd_1 site is given by the following expression:

$$\mathbf{E}_{\text{eff,Cd}_1}=\mathbf{E}+q_{11}\mathbf{P}_{\text{Cd}_1}+q_{12}\mathbf{P}_{\text{Cd}_2}+q_{13}\mathbf{P}_{\text{S}_1}+q_{14}\mathbf{P}_{\text{S}_2}. \tag{4}$$

The $\mathbf{P}$'s are the dipole moments per unit volume arising from the atomic displacements and the electronic polarization. The q tensors contain the lattice sums for dipole arrays. The lattice sums were calculated using the method described by Kittel.[4] For transverse vibrations polarized along the z direction in the ideal wurtzite structure, we obtain for the zz tensor components

$$\begin{aligned}q_{11}&=-\ 7.220+4\pi/3,\\ q_{12}&=\ \ 7.230+4\pi/3,\\ q_{13}&=\ 14.40\ +4\pi/3,\\ q_{14}&=-14.00\ +4\pi/3.\end{aligned}$$

For vibrations polarized along the x (or y) direction, we obtain for the tensor components

$$\begin{aligned}q_{11}&=\ \ 3.610+4\pi/3,\\ q_{12}&=-3.615+4\pi/3,\\ q_{13}&=-7.20\ +4\pi/3,\\ q_{14}&=\ \ 7.00\ +4\pi/3.\end{aligned}$$

We note that there are large deviations from the simple $4\pi/3$ values encountered in the $GaAs_yP_{1-y}$ system.

In the evaluation of effective-field expressions, Cohen has pointed out that it is not really valid to add the atomic-displacement polarization and electronic polarization in the way suggested by Eq. (2).[5] In fact, we do not want the effective field at the equilibrium position of the ion, but at the center of the ion, which is displaced from the equilibrium position because of the vibrationary motion of the ion. Now, as far as a Cd_1 ion is concerned, all other Cd_1 and Cd_2 ions for a $\mathbf{q}\approx 0$ infrared mode move in phase with it. The Cd sublattice moves as if it is rigid. Hence no dipolar field is experienced by Cd ions due to the vibration of other Cd ions. There may, of course, be a contribution from the electronic polarization of the Cd ions. If we further take into account the fact that for the infrared-active modes $\mathbf{P}_{\text{Cd}_1}=\mathbf{P}_{\text{Cd}_2}$, and $\mathbf{P}_{\text{S}_1}=\mathbf{P}_{\text{S}_2}$, we can write Eq. (4) for the effective field at the center of an arbitrary Cd ion using Cohen's method:

$$\begin{aligned}\mathbf{E}_{\text{eff,Cd}}=\mathbf{E}&+(q_{11}+q_{12})\mathbf{P}_{\text{el,Cd}}\\ &+(q_{13}+q_{14})(\mathbf{P}_{\text{el,S}}+\mathbf{P}_{\text{d,S}}),\end{aligned} \tag{5}$$

where we use the subscripts el and d to denote electronic and displacement components of the polarization. We have then

$$\mathbf{P}_{\text{el,Cd}}=\tfrac{1}{2}N\alpha_{\text{Cd}}\mathbf{E}_{\text{eff,Cd}},\quad \mathbf{P}_{\text{el,S}}=\tfrac{1}{2}N\alpha_{\text{S}}\mathbf{E}_{\text{eff,S}},$$

and $\mathbf{P}_{\text{d,S}}=\tfrac{1}{2}Ne(\mathbf{w}_{\text{Cd}}-\mathbf{w}_{\text{S}})$. We note again that N is the number of ion pairs per unit volume. The appearance of $(\mathbf{w}_{\text{Cd}}-\mathbf{w}_{\text{S}})$ in the last definition rather than $\mathbf{w}_{\text{S}}$ arises from the fact that the field is evaluated at the displaced center of the Cd ion, rather than at the equilibrium position.[5]

Substituting the zz tensor components of q_{ij} in Eq. (5), we obtain

$$\begin{aligned}E_{\text{eff,Cd}}(z)=E(z)&+(4\pi/3+0.005)N\alpha_{\text{Cd}}E_{\text{eff,Cd}}(z)\\ &+(4\pi/3+0.2)N\alpha_{\text{S}}E_{\text{eff,S}}(z)\\ &+(4\pi/3+0.2)Ne(z)[w_{\text{Cd}}(z)-w_{\text{S}}(z)]\end{aligned} \tag{6}$$

for the effective field in the z direction. For the effective field on the sulphur (or Se) ion, we similarly find

$$\begin{aligned}E_{\text{eff,S}}(z)=E(z)&+(4\pi/3+0.2)N\alpha_{\text{Cd}}E_{\text{eff,Cd}}(z)\\ &+(4\pi/3+0.005)N\alpha_{\text{S}}E_{\text{eif,S}}(z)\\ &+(4\pi/3+0.2)Ne[w_{\text{Cd}}(z)-w_{\text{S}}(z)].\end{aligned} \tag{7}$$

Note the finite, but small, deviation of the Lorentz factor from $4\pi/3$ for these infrared-active modes. For transverse vibrations polarized in the x or y directions, the dipole term $(4\pi/3+0.005)$ becomes $(4\pi/3-0.0025)$, and $(4\pi/3+0.20)$ becomes $(4\pi/3-0.10)$. For the other optic modes of the wurtzite structure where the two like ions in the unit cell do not vibrate in phase, much larger contributions from the third term in Eq. (3) would be obtained.

As mentioned, all these considerations are based on the existence of point dipoles at the equilibrium sites of the lattice. Whereas this assumption is generally considered to be a reasonable one for the electrons in such ionic compounds as the alkali halides, Brodsky and Burstein[2] have suggested that for the III-V and II-VI compounds the electron cloud around each ion is not entirely localized, but has considerable overlap with adjacent cells. As in Paper I, we approximate this

[3] M. Born and K. Huang, *Dynamical Theory of Crystal Lattices* (Clarendon Press, Oxford, England, 1954), Chap. 2, Sec. 9.

[4] J. C. Slater, Phys. Rev. **78**, 748 (1950); H. Kornfeld, Z. Physik **22**, 27 (1924); C. Kittel, *Solid State Physics* (John Wiley & Sons, Ltd., London, 1956), p. 193 and Appendix A.

[5] M. H. Cohen, Phys. Rev. **84**, 368 (1951).

behavior by dividing the effective ionic charge e into two parts:

$$e=e_l+e_{nl}.$$

e_{nl}, the nonlocal part of the effective charge, represents the overlapping part of e. For simplicity, we extend this latter charge over the whole crystal so that it contributes a uniform polarization when the ion moves and interacts only with the uniform electric field E. In addition, we also take the polarizable electron cloud (which determines α) to be entirely of an extended nature.[2] Thus P_{el} is determined by E and not E_{eff}. Using these considerations, Eqs. (6) and (7) become

$$E_{eff}(z)=E(z)+(4\pi/3+0.2)P_{loc}(z) \tag{8a}$$

for either Cd or S.

Similarly, for the other polarization we obtain

$$E_{eff}(x)=E(x)+(4\pi/3-0.1)P_{loc}(x). \tag{8b}$$

E_{eff} is the effective field experienced by the local charge, and is the same at all ion centers. In these expressions, P_{loc} is the atomic-displacement polarization arising from the local effective charge

$$P_{loc}=Ne_l(w_+-w_-). \tag{9}$$

The dipoles associated with the nonlocal charge do not contribute to the dipolar field as mentioned above. We now apply these considerations of the effective field to our basic equations for the displacement and polarization [Eqs. (1) and (2)]. Substituting Eqs. (8) and (9) into Eqs. (1) and (2), we obtain

$$u(i)=-\left[\frac{k(i)}{\bar{m}}-\left(\frac{4\pi}{3}+c\right)\frac{Ne_l^2}{\bar{m}}\right]u(i)+\frac{e(i)}{\bar{m}}E(i), \tag{10}$$

$$P(i)=N[e_l+e_{nl}(i)]u(i)+N(\alpha_++\alpha_-)E(i), \tag{11}$$

where $c=0.20$ if i denotes the direction parallel to the c axis, and $c=-0.10$ for the direction perpendicular to the c axis. We assume that the anisotropy in the optic-mode strengths is entirely due to the nonlocal or distributed portion of the effective charge. In going from the cubic zinc-blende structure discussed in I to the wurtzite structure of $CdSe_ySe_{1-y}$, Eqs. (10) and (11) for the long-wavelength infrared-active modes take account of the anisotropy through direction-dependent force constants and charges. In addition, the corrections to the $4\pi/3$ Lorentz field which are included in the equations are anisotropic, though small for these modes. Equations (10) and (11) are used in the discussion of pure CdS and pure CdSe, and are the equations to be generalized for the mixed crystals.

C. The Dielectric Constant and Reflectivity for One Mode

Because $\mathbf{q}\approx 0$, the displacements and fields have only an $\exp(i\omega t)$ dependence. Using this time dependence in Eq. (10), we obtain

$$\omega^2(i)u(i)=\left[\frac{k(i)}{\bar{m}}-\left(\frac{4\pi}{3}+c\right)\frac{Ne_l^2}{\bar{m}}\right]u(i)-\frac{e}{\bar{m}}E(i). \tag{12}$$

The TO frequencies for the two polarizations are given by

$$\omega_{TO}^2(i)=\frac{k(i)}{m}-\left(\frac{4\pi}{3}+c\right)\frac{Ne_l^2}{\bar{m}}.$$

To obtain the dielectric constant we use

$$P(i)=\frac{\epsilon(i)-1}{4\pi}E(i). \tag{13}$$

Eliminating u and E from Eq. (11), and introducing an *ad hoc* damping constant $\Gamma(i)$, we find

$$\epsilon(i)=\epsilon(i)_\infty+\frac{4\pi Ne^2(i)}{\bar{m}[\omega_{TO}^2(i)-\omega^2-i\Gamma(i)\omega\omega_{TO}(i)]}. \tag{14}$$

The strength of a single active mode is defined in terms of the difference between the high- and low-frequency dielectric constants:

$$\begin{aligned}4\pi\rho(i)&\equiv\epsilon(i)_0-\epsilon(i)_\infty\\&=4\pi Ne^2(i)/\bar{m}\omega_{TO}^2(i).\end{aligned} \tag{15}$$

Finally, we obtain the reflectivity at normal incidence as a function of the dielectric constant from the Fresnel equation:

$$R(i)=\left|\frac{[\sqrt{\epsilon(i)}]-1}{[\sqrt{\epsilon(i)}]+1}\right|^2. \tag{16}$$

This calculated reflectivity may be compared with experiment to determine the mode parameters ϵ_∞, ω_{TO}, $4\pi\rho$, and Γ. Starting with trial parameters, these are adjusted until a best fit of the experimental reflectivity is obtained. The general procedure of reflectivity fitting is discussed in the literature.[6,7]

Before discussing the experiments and the mixed-crystal model with its eight infrared modes, we note that for the one-mode case of a pure crystal, there are only two experimentally measurable quantities, ω_{TO} and $4\pi\rho$, but three unknown parameters, k, e_l, and e_{nl}. Hence Burstein's suggestion that the charge has a local and nonlocal portion cannot be verified from a study of the reflectivity of such crystals. Later, we shall see that our study of the reflectivity of mixed crystals for several concentrations will enable us to obtain e_l and e_{nl}. We shall then conclude that our work supports Burstein's suggestion.

[6] W. G. Spitzer and D. A. Kleinman, Phys. Rev. **121**, 1324 (1961).
[7] A. S. Barker, Jr., Phys. Rev. **132**, 1474 (1963).

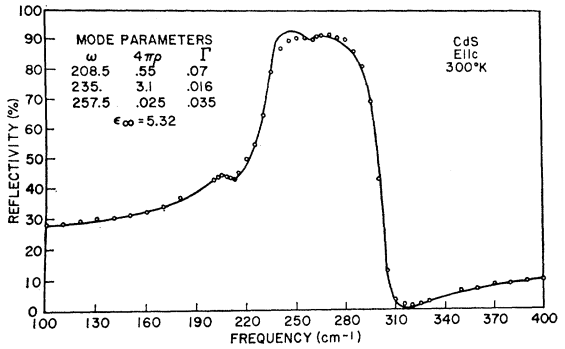

FIG. 3. Classical oscillator fit (solid line) of far-infrared reflectivity spectrum of CdS at 300°K with $\mathbf{E}\|$ (c axis). Open circles are experimental points.

EXPERIMENTAL WORK

A. Sample Preparation

A number of single crystals of $CdSe_ySe_{1-y}$, representative of the entire composition range, were purchased from the Clevite Research Center. These crystals have very low carrier concentrations (about 10^4 cm^{-3})[8,9]; hence, free-carrier effects on the measured reflectivities can be completely ignored. All crystals were grown from the vapor phase at temperatures near 1200°C, using sintered slugs of mixed powdered CdS and CdSe as starting material.[8]

The lattice constant (a_0) of this alloy varies almost linearly with composition[9] from its value for CdS (4.125 Å) at $y=0$ to its value for CdSe (4.292 Å) at $y=1$. Use was made of this property to determine the average composition of the crystals, i.e., the value of y. The Bragg peak from the $(10\bar{1}0)$ or $(11\bar{2}0)$ planes was measured using a double-crystal x-ray spectrometer, and the lattice constant and composition were calculated from this. The $(10\bar{1}0)$ or $(11\bar{2}0)$ lines for both the mixed crystals and the parent crystals had widths at half-maximum height of about 10′. No variation in composition could be detected by measuring the Bragg reflections from different portions of a given crystal. We estimate the determined composition to be precise to within 1%.

Since wurtzite-type crystals are optically uniaxial, the reflectivity measurements were made with polarized light. Each crystal had a polished face of at least 1 cm×1 cm containing the c axis. This allowed us to measure $R(\perp)$ and $R(\|)$ from the same face of the crystal by either rotating the polarizer or the crystal through 90°.

All samples were mechanically polished using a 0.3-μ aluminum-oxide abrasive. In addition, chemical polishing of some of these crystals was done to remove surface damage. In this procedure, an etch was applied to the surface via a rotating disk covered with a fine-nap cloth to prevent abrasions. We were only partially successful in obtaining good finishes with this etch technique. The etch used for CdS was a 30% solution of HCl in water, and it yielded a good mirror-like finish. However, the etch rate of the mixed crystals and of CdSe in even stronger concentrations of HCl in water was much slower. Of the various materials tried, a 60% solution of HCl in water provided the best results, even though these were in no way comparable with those obtained for CdS. The long etch time required to give a good polish for the mixed crystals caused a rounding of the edges, with resultant loss of flatness of the surface. We tried to strike a compromise between a good polish, which requires a long etch, and this loss of flatness.

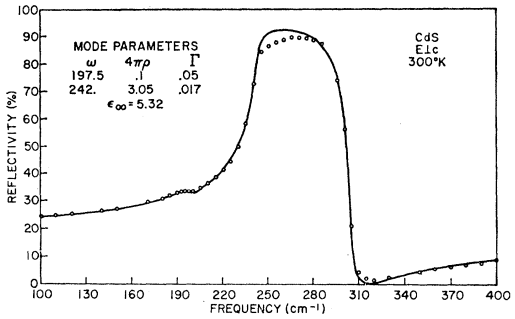

FIG. 4. Classical oscillator fit (solid line) of far-infrared reflectivity spectrum of CdS at 300°K with $\mathbf{E}\perp$ (c axis). Open circles are experimental points.

In the region of the spectrum where the penetration depth of the incident radiation is of the order of a micron, i.e., within the reststrahlen band, the measured reflectivity may be strongly surface-dependent.[7] The chemically polished CdS crystals showed an increased reflectivity in that region of the spectrum over the mechanically polished crystals. Since the reflectivity elsewhere in the spectrum was the same for both types of surface, this indicated that the etching had removed some or all of the surface damage. For CdSe and the mixed crystals, the reflectivity results for the two types of surface were not substantially different with allowances for the nonflat surface of the crystals.

B. Reflectivity Measurements

The infrared reflectivity spectra were measured using a Perkin-Elmer single-beam grating spectrometer over the frequency range from 100 to 400 cm^{-1}. For the low-temperature measurements, the samples and reference mirror were mounted on a sliding holder attached to the helium cold finger of an optical Dewar. A room-temperature polyethylene window was used which, together with a 77°K shield, resulted in a 15°K sample temperature for the cooled runs. The general method of taking data has been discussed by others.[6] A resolution

[8] L. R. Shiozawa (private communication, 1966).
[9] L. R. Shiozawa, S. Devlin, and J. M. Jost, Ninth Quarterly Progress Report, 1959, Contract No. AF33(616)3923, Clevite Research Center (unpublished).

of 2.5 cm^{-1} was maintained over the entire frequency range. The absence of appreciable systematic errors in the equipment was verified by comparing our reflectivity measurements on more standard materials with those made by others. Agreement was always within 1% reflectivity. The effect of random errors was determined by rerunning certain measurements after repositioning the specimen. Agreement between different runs on the same specimen was again obtained to within 1%.

DISCUSSION OF EXPERIMENTAL RESULTS

A. CdS

Room-temperature measurements are shown in Figs. 3 and 4 for the electric vector polarized parallel and perpendicular to the c axis, respectively. The open circles are the experimental data, and the solid line is an oscillator fit to the reflectivity. The mode parameters are listed in the figures. The A_1 and E_1 TO frequencies of the main modes are quite close (235 and 242 cm^{-1}), showing that this material is only slightly anisotropic. These frequencies agree with those obtained from transmission studies by Balkanski *et al.*[10] and are in reasonable agreement with Collins's reflectivity measurements made with unpolarized light.[11] In addition to the fundamental A_1 and E_1 modes, weaker modes are observed at 208.5 cm^{-1} for $\mathbf{E}\|c$ and at 197.5 cm^{-1} for $\mathbf{E}\perp c$. Similar modes are also observed in the transmission studies of Balkanski *et al.*, namely, at 210 and 200 cm^{-1}, respectively. They conclude from the relatively large integrated intensity, as well as the relatively small temperature dependence, of these modes that they are due to normally infrared-inactive but fundamental modes of the crystal. Poulet and Mathieu[12] have observed these modes at 212 cm^{-1} in their Raman-scattering studies. Recent work was done on the Raman spectra of CdS by Tell *et al.*[13] They observe a mode at 207 cm^{-1}. However, from symmetry considerations and the observed temperature dependence, they assign this mode to a multiphonon process in contrast to Balkanski *et al.*[14]

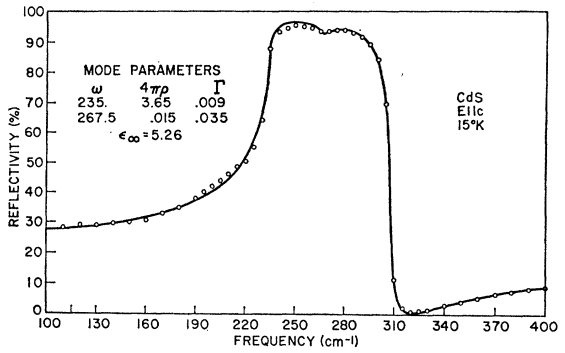

FIG. 5. Classical oscillator fit (solid line) of far-infrared reflectivity spectrum of CdS at 15°K with $\mathbf{E}\|(c$ axis). Open circles are experimental points.

The absorption coefficient corresponding to a fundamental mode is temperature-independent. For absorption due to two-phonon transitions, the temperature dependence goes as $1+n_1+n_2$ for summation bands, and as n_1-n_2 for difference bands.[13] Here n_j is the average number of phonons in a quantum state j given by

$$n_j=(e^{h\nu_j/kT}-1)^{-1}.$$

We have measured the reflectivity of CdS at 15°K. The results for both polarizations are shown in Figs. 5 and 6. The data show almost complete absence of the 208 and 197 modes. A good fit to the spectrum requires a strong mode at 235 cm^{-1} plus a very weak mode on top of the reststrahlen band. The temperature dependence of the mode at 208 cm^{-1} can be calculated by assuming it to be due to a difference band of phonons with frequencies 252 and 44 cm^{-1}, respectively. These latter are Tell's assignments of the two E_2 Raman-active modes. We must, of course, assume that these phonon branches have very little $\mathbf{q}$ dependence because the Raman effect measures the phonons at $\mathbf{q}\approx 0$, while the two-phonon band is weighted by the high density of states near the zone boundary. The calculation shows a reduction in strength of the 208 cm^{-1} mode by a factor of about 250 upon cooling from 300 to 15°K. The almost total absence of the mode at 15°K in our experimental work thus confirms Tell's conclusion that the 208-cm^{-1} mode is due to multiphonon processes.

Turning now to the main modes, we observe a considerable increase in strength of the A_1 mode when the temperature is lowered to 15°K. In fact, the total strength of the two modes at room temperature (Fig. 3)

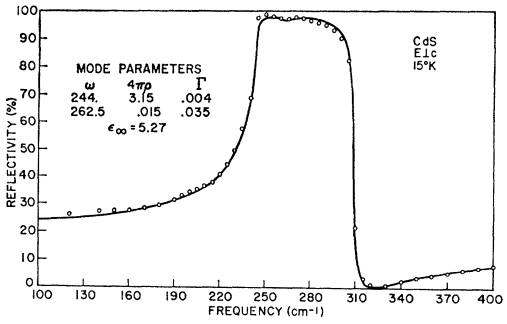

FIG. 6. Classical oscillator fit (solid line) of far-infrared reflectivity spectrum of CdS at 15°K with $\mathbf{E}\perp$ (c axis). Open circles are experimental points.

[10] M. Balkanski, J. M. Besson, and R. LeToulec, in *Proceedings of the Seventh International Conference on Semiconductors, Paris, 1964* (Academic Press Inc., New York, 1964), p. 1091.

[11] R. J. Collins, J. Appl. Phys. **30**, 1135 (1959).

[12] H. L. Poulet and J. P. Mathieu, Ann. Phys. (Paris) **9**, 549 (1964).

[13] B. Tell, T. C. Damen, and S. P. S. Porto, Phys. Rev. **144**, 771 (1966).

[14] See, for example, M. Balkanski *et al.*, in *Proceedings of the Seventh International Conference on Semiconductors, Paris, 1964* (Academic Press Inc., New York, 1964), p. 1021.

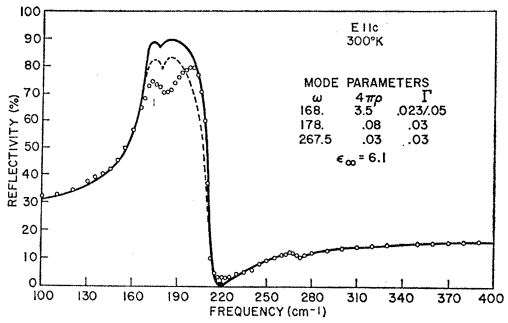

FIG. 7. Classical oscillator fits (solid and dotted line) of far-infrared reflectivity spectrum of $CdSe_{0.985}S_{0.015}$ at 300°K with $\mathbf{E}\|(c$ axis). The difference between the solid and dotted line is in the damping constant employed for the main mode. Open circles are the experimental points.

is 0.55+3.1, and equals the strength of the reststrahlen band at 15°K (Fig. 5). Since one would expect the fundamental mode to be temperature-independent, this increase in strength is not understood. A similar situation occurs with the other polarization ($\mathbf{E}\perp c$). At 300°K we find two modes of strength 3.05 and 0.1, respectively. At 15°K a single mode of strength 3.15 exists. We note a considerable decrease in damping of the main mode with cooling. The TO frequencies and the high-frequency dielectric constants, however, are found to be relatively temperature-independent.

Very weak modes appear on top of the reststrahlen bands at both temperatures. Their frequencies suggest that they are normally infrared-inactive, but Raman-active modes. Tell's assignment of one E_2 mode at 252 cm^{-1} agrees reasonably well with the value of 257.5 cm^{-1} found at 300°K with the E vector polarized parallel to the c axis. The fundamental mode parameters and derived constants are summarized in Table I. The ion-pair density N listed in this table is based on the room-temperature values of the lattice constants. At 15°K it should be slightly larger, though no measurements of the lattice constants at liquid-helium temperature are available. The change can hardly be significant, however, in view of the small expansion coefficient this material has at room temperature.

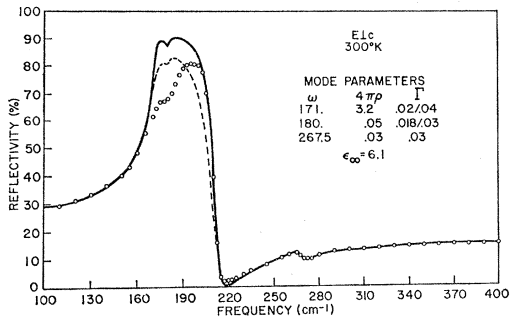

FIG. 8. Classical oscillator fits (solid and dotted lines) of far-infrared reflectivity spectrum of $CdSe_{0.985}S_{0.015}$ at 300°K with $\mathbf{E}\perp(c$ axis). The difference between the solid- and dotted-line fits is in the damping constants employed for the main mode. Open circles are the experimental points.

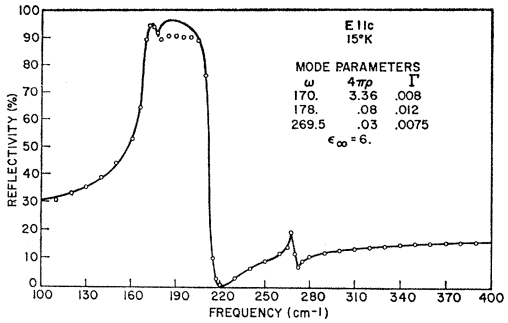

FIG. 9. Theoretical fit, based on model (solid line) of far-infrared reflectivity spectrum of $CdSe_{0.985}S_{0.015}$ at 15°K with $\mathbf{E}\|(c$ axis). Open circles are experimental points.

B. CdSe

When the far-infrared reflectivity of so-called "pure" CdSe was measured, a weak mode near 270 cm^{-1}, well above the reststrahlen region, was found. Experience with the model of vibrations in the mixed crystal suggested the presence of S in the lattice. This was confirmed by measurement of the x-ray fluorescence of the crystal. In the fluorescence analysis, the characteristic K_α line of sulphur was excited, and its intensity compared with the sulphur line in mixed crystals of $CdSe_ySi_{1-y}$ of known sulphur content. All of our "pure" CdSe was found to contain 1 to 2% S. A specimen containing $1\frac{1}{2}$% sulphur was finally used in the reflectivity measurements presented here (Figs. 7 to 10). Besides the weak mode at 270 cm^{-1}, the presence of sulphur in the lattice causes fine structure on top of the CdSe reststrahlen band. This fine structure is a direct consequence of the mixed-crystal model, and is exactly like the fine structure seen on the reststrahlen bands in the $GaAs_yP_{1-y}$ system. The reflectivity spectra for the two polarizations at 15 and 300°K are shown in Figs. 7–10.

The theoretical fits (solid and dotted lines) for CdSe are based in part on the mixed-crystal model because of the presence of sulphur. This model was applied to the case $\mathbf{E}\|(c$ axis) at 15°K for which the strengths and

TABLE I. Mode parameters and related constants of CdS at 300°K and at 15°K.

	ω_{TO} (cm^{-1})	ϵ_∞	$4\pi\rho$	Γ	e (10^{-10} esu)	N (10^{22} cm^{-3})
CdS 300°K $\mathbf{E}\|c$	235.0	5.32	3.1	0.016	10.0	2.01
CdS 300°K $\mathbf{E}\perp c$	242.0	5.32	3.05	0.017	10.2	2.01
CdS 15°K $\mathbf{E}\|c$	235.0	5.27	3.65	0.009	10.87	2.01
CdS 15°K $\mathbf{E}\perp c$	244.0	5.27	3.15	0.004	10.3	2.01

TABLE II. Mode parameters and related constants of CdSe. I, our measurements; II, Geick's measurements.

	ω_{TO} (cm^{-1})		ϵ_∞		$4\pi\rho$		Γ		e (10^{-10} esu)		N (10^{22} cm^{-3})
	I	II	I	II	I	II	I	II	I	II	
CdSe 300°K E‖	168	166	6.1	6.3	3.62	3.86	0.025–0.05	0.048	11.2	11.5	1.78
CdSe 100°K E‖		168		6.3		3.61		0.035		11.2	1.78
CdSe 15°K E‖	170		6.0		3.5		0.012		11.15		1.78
CdSe 300°K E⊥	171	172	6.1	6.2	3.3	3.1	0.02–0.04	0.042	10.9	10.6	1.78
CdSe 100°K E⊥		175		6.2		2.95		0.028		10.55	1.78
CdSe 15°K E⊥	173.5		6.1		3.18		0.006		10.85		1.78

frequencies, shown in Fig. 9, were calculated. For the other three cases, we adjusted the mode parameters to obtain a best fit. The results are good everywhere, except on top of the reststrahlen bands, where, especially for the 300°K measurements, a good fit cannot be attained. In Figs. 7 and 8, we have shown the effect of increasing the damping constant (dotted line). This lowers the theoretical reflectivity on top of the bands, but makes the fit worse elsewhere. Recently, the reflectivity spectra of CdSe have also been reported by Geick *et al.*[15] These workers encounter exactly the same problem with their room-temperature fits.

The poor fit on top of the reststrahlen bands is believed to be due in part to the fact that our *ad hoc* damping constant Γ takes account of energy absorption only in the simplest way. When the temperature is reduced, the damping decreases, and any discrepancies between our constant value for Γ and its actual, frequency-dependent, value become less pronounced. The fit of the low-temperature measurements is considerably better. Since our results for 98 to 99% CdSe are easily extrapolated to 100%, we can compare our results with those obtained by Geick *et al.* This is done in Table II. There is substantial agreement between the analyses, although there is some discrepancy (6%) in the strength of the modes. Again we notice that the strength of the *Reststrahlen* band is not independent of temperature; in this crystal it decreases upon cooling. In addition, there is a measurable increase of the TO frequencies on cooling in contrast to the behavior of CdS.

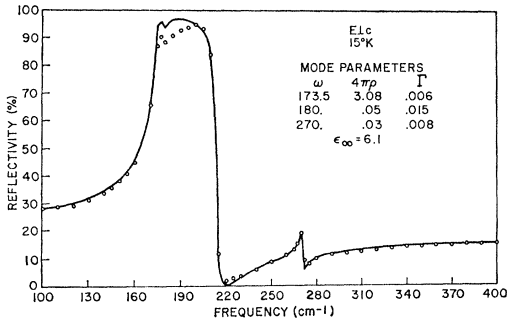

FIG. 10. Classical oscillator fit (solid line) of far-infrared reflectivity spectrum of $CdSe_{0.985}S_{0.015}$ at 15°K and $\mathbf{E}\perp$ (c axis). Open circles are experimental points.

[15] R. Geick, C. H. Perry, and H. Mitra, J. Appl. Phys. **37**, 1994 (1966).

C. $CdSe_ySe_{1-y}$

In Figs. 11, 12, and 13, the room-temperature reflectivity spectra of three mixed crystals are shown for both the E vector parallel to, and the E vector perpendicular to the c axis. In all cases there is very little difference between the two polarizations. The high-frequency dielectric constants are the same for the two polarizations at all values of y, as is evident from the identical reflectivities near 400 cm^{-1}. Since the sum of the strengths of the lattice-vibration modes is smaller for $\mathbf{E}\perp$ (c axis), the low-frequency dielectric constants are lower for this polarization than for $\mathbf{E}\|$ (c axis). These reflectivity spectra demonstrate that just as in the parent crystals, the alloys are only slightly anisotropic as far as their lattice-vibrational properties are concerned. Both polarizations show similar fine structure near the reststrahlen bands.

The reflectivity spectra of the mixed crystals were measured at 15°K for the following compositions: $y=0.26$, 0.53, 0.75, and 0.985. In Fig. 14 we have superimposed the spectra for these crystals on the $\mathbf{E}\|$ (c axis) spectrum of CdS. The characteristic features are similar to those of the $GaAs_yP_{1-y}$ system, reported on in Paper I, though we note the following differences:

(1) The frequency shift of the bands is quite different from that encountered in $GaAs_yP_{1-y}$. The high-frequency band here appears to shift to higher frequencies with increasing y. A more careful examination, however, will reveal that only the strongest mode shifts by about 23 cm^{-1}, from 235 cm^{-1} at $y=0$ to 258 cm^{-1} at $y=1$. The three weaker modes giving the fine

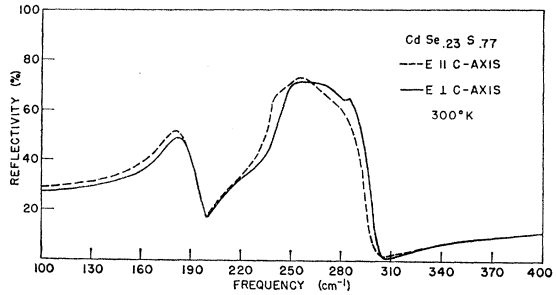

FIG. 11. Experimentally determined far-infrared reflectivity spectra of $CdSe_{0.23}S_{0.77}$ at 300°K. Solid line is smooth line drawn through experimental points for $\mathbf{E}\|$ (c axis). Dashed line is for $\mathbf{E}\|$ (c axis).

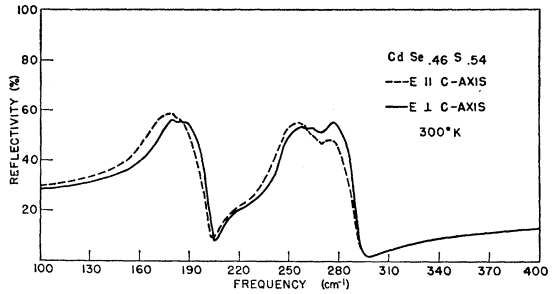

FIG. 12. Experimentally determined far-infrared reflectivity spectra of $CdSe_{0.46}S_{0.54}$ at 300°K. Solid line is smooth line drawn through experimental points for $\mathbf{E}\perp$ (c axis). Dashed line is for $\mathbf{E}\parallel$ (c axis).

structure in the high-frequency band still shift to lower frequencies by from 5 to 10 cm^{-1}.

(2) In $GaAs_yP_{1-y}$, the weaker modes in the low-frequency band have lower frequencies than the main mode. In $CdSe_yS_{1-y}$, they have higher frequencies, causing the structure on the low-frequency band which is especially noticeable at high values of y.

That the fine structure on each reststrahlen band is not surface-dependent was confirmed by comparing etched and mechanically polished specimens. Neither is the structure temperature-dependent, as comparison between Figs. 11–13 with 14 reveals. The decrease in damping when the temperature is lowered does make the fine structure more pronounced in the low-temperature spectra.

APPLICATION OF THE MIXED-CRYSTAL MODEL TO $CdSe_yS_{1-y}$

A. Basic Units and Force Constants

Each Cd ion has four nearest neighbors which, in the mixed crystal, may be either Se or S. The arrangement of these ions around the Cd ion is like that in $GaAs_yP_{1-y}$, i.e., the Se and S ions form a tetrahedron with the Cd ion at the center. As in I, therefore, the entire lattice is built up from five basic units, each unit containing two ions, viz. a Cd ion and one quarter of the S or Se ions located on each of the nearest-neighbor sites. These units are shown in Fig. 15.

As far as nearest neighbors are concerned, we have a situation identical to that described in I. We introduce five Cd-ion sublattice coordinates $w_{Cd}(i)$, $i=1$ to 5, to take account of the five possible nearest-neighbor environments of the Cd ions. Similarly, we introduce $w_{Se}(i)$, $i=1$ to 4, and $w_S(i)$, $i=2$ to 5, recognizing again that unit 1 does not contain any S ions, and unit 5 does not contain any Se ions. The interaction between a Cd ion and a Se ion will again, in part, depend on the other three ions associated with the Cd ion. That is, it will depend on whether the Cd is at the center of unit type 1, 2, 3, or 4. This leads to the introduction of four Cd-Se nearest-neighbor force constants $k_1(i)$, $i=1$ to 4, and similarly four Cd-S nearest-neighbor coordinates $k_2(i)$, $i=2$ to 5. To take account of the sharing of negative ions by neighboring units, we introduce the force constants k_7 and k_8 between the Cd ions in unit i and the Se and S ions in surrounding units j.

The second-neighbor interactions arise in the mixed crystal because like ions belonging to different units can vibrate out of phase. Although the distribution of second neighbors in $CdSe_yS_{1-y}$ is not the same as it is in $GaAs_yP_{1-y}$, this does not affect the formalism. We again consider deviations from a random distribution of negative ions up to nearest neighbors of the Cd ions only. This means that we will assume that all negative ions see the same set of second neighbors, viz. the average set of $12y$ Se ions and $12(1-y)$ S ions. The factor 12 and any geometrical factors are again included in the force constants, which are k_3 for Se-Se, k_4 for Se-S, k_5 for S-S, and k_6 for Cd-Cd interactions. The nonisotropic distribution of second neighbors will, in principle, make these constants different for the two principal directions of the crystal ($\parallel$ and $\perp$ to the c axis). The nomenclature, aside from the inclusion of the $\parallel$ and $\perp$ dependences, is the same as in I.

B. Probability of Occurrence of Basic Units

The basic relations for the probability of finding a Se ion next to another Se ion (P_{SeSe}), and for finding a S ion next to another S ion (P_{SS}), for a mixed crystal with Se concentration y are

$$P_{SeSe}=y+\beta(1-y), \tag{17}$$

$$P_{SS}=(1-y)+\beta y. \tag{18}$$

These are the same equations as Eqs. (1) and (2) in I with different subscripts. Note that Eq. (17) shows that the effect of the clustering parameter β is to increase the probability of finding a Se ion next to a given Se ion. The methods introduced in I allow us to define the probabilities of occurrence of unit type i, using Eqs. (17) and (18). These latter probabilities play a key role in determining the strengths of the mixed-crystal optic modes. Paper I can be consulted for details.

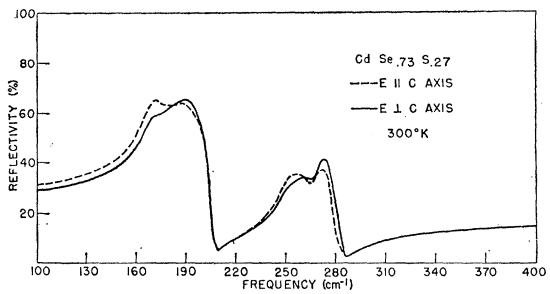

FIG. 13. Experimentally determined far-infrared reflectivity spectra of $CdSe_{0.73}S_{0.27}$ at 300°K. Solid line is smooth line drawn through experimental points for $\mathbf{E}\perp$ (c axis). Dashed line is for $\mathbf{E}\parallel$ (c axis).

C. Dielectric Constant

In writing the potential energy and equations of motion for $GaAs_yP_{1-y}$, the direction of the externally applied field was immaterial since the crystal was optically isotropic.[1] In $CdSe_ySi_{1-y}$, we take the field direction to be along the c axis or perpendicular to it, depending on the polarization being considered. The small difference in frequencies of the various lattice-vibrational modes between the two polarizations will lead to slightly different sets of force constants for $\mathbf{E}\|$ and $\mathbf{E}\perp$ (c axis). The difference in strengths of the modes for the two polarizations leads to different effective ionic charges for $\mathbf{E}\|$ and $\mathbf{E}\perp$ (c axis), as was already discussed (see Tables I and II).

For each direction of polarization, we can now write down equations of motion and an expression for the dielectric polarization identical to those presented in I with a mere change of subscripts from g, a, p to Cd, Se, S. The expression for the effective field must, however, be replaced by

$$\mathbf{E}_{\text{eff}}=\mathbf{E}+(4\pi/3+c)\mathbf{P}_{\text{loc}}, \tag{19}$$

where $c=0.20$ for $\mathbf{E}\|$ (c axis) and $c=-0.10$ for $\mathbf{E}\|$ (c axis). Taking the same correction to the $4\pi/3$ coefficient in the mixed crystals as in the parent crystals is consistent with the basic assumption of our model that each anion site is occupied by the virtual ion

$$x(i)\text{Se}+[1-x(i)]\text{S},$$

where $x(i)=1, \frac{3}{4}, \frac{1}{2}, \frac{1}{4}$, or 0 for $i=1$ to 5 (units 1 to 5).

The solution of the dynamical matrix to obtain the eigenfrequencies and mode strengths then proceeds as outlined in the Appendix of I, yielding the following expression for the dielectric constant:

$$\epsilon(\omega,y,\beta,i)=\epsilon_\infty+\sum_{j=i}^{8}\frac{4\pi\rho_j\omega_j^2}{\omega_j^2-\omega^2-i\omega\Gamma_j\omega_j}. \tag{20}$$

The implicit dependence of ϵ on the composition y, the clustering parameter β, and the direction i, is indicated since both the mode strengths $4\pi\rho$ and the mode frequencies ω_j depend on these.

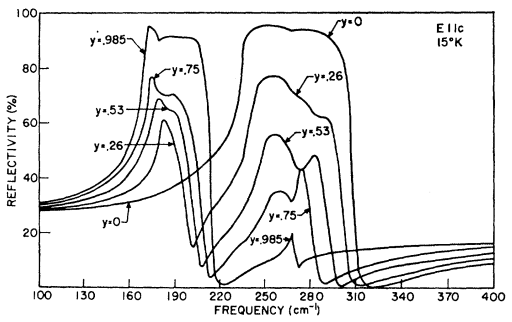

FIG. 14. Experimentally determined far-infrared reflectivity spectra of CdS and four mixed crystals of $CdSe_ySi_{1-y}$ at 15°K with $\mathbf{E}\|$ (c axis). A smooth line was drawn through experimental points.

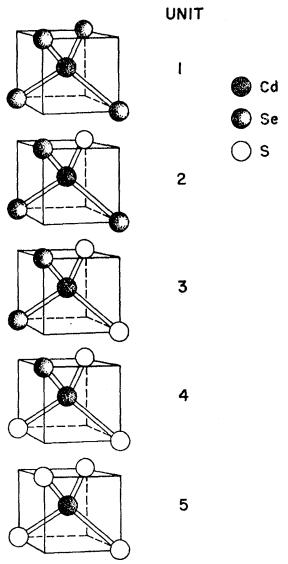

FIG. 15. Basic units of nearest-neighbor ions around a Cd ion site.

D. Theoretical Fit of Reflectivity Spectra

The actual calculations to obtain a theoretical fit of the experimental mixed-crystal spectra were performed for the $\mathbf{E}\|$ (c axis) measurements at 15°K. As mentioned previously, there is considerable anharmonic structure in the room-temperature spectra of CdS. Our model, being harmonic, does not give any information on the y dependence of that structure. The reflectivity spectra of CdS at 15°K can be fit adequately with a single oscillator, thus allowing straightforward application of the model to CdS and the entire range of alloys.

Preliminary trial fits for the $\mathbf{E}\perp$ (c axis) mixed-crystal spectra taken at 15°K indicate that similar results can be obtained for this polarization by choosing a slightly different set of force constants and charges. A complete evaluation of the model parameters was not carried out, however, for $\mathbf{E}\perp$ (c axis).

The known physical constants used in the calculations of the model are listed in Table III. Starting values for the local charges were obtained as in I from the known compressibilities of CdSe and CdS. The TO frequency

TABLE III. Physical constants used in the calculations of the model for $CdSe_ySi_{1-y}$ at 15°K and $\mathbf{E}\|c$.

	Constant	Value
Mass	m_{Cd}	18.65×10^{-23} g
	m_{Se}	13.10×10^{-23} g
	m_{S}	5.33×10^{-23} g
Charge	e_{Se}	11.15×10^{-10} esu
	e_{S}	10.87×10^{-10} esu
Dielectric constant	ϵ_∞(CdSe)	6.0
	ϵ_∞(CdS)	5.27
Lattice constant	a_0(CdSe)	4.293 Å
	a_0(CdS)	4.125 Å
Ion-pair density	N_{CdSe}	1.78×10^{22} cm^{-3}
	N_{CdS}	2.015×10^{22} cm^{-3}

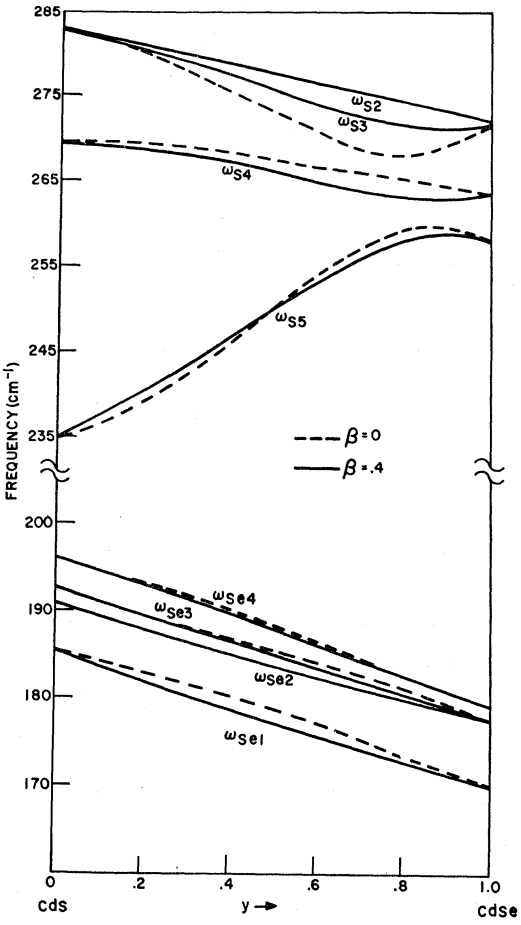

FIG. 16. Mode frequencies versus composition (y), computed from the model for $\beta=0$ and $\beta=0.4$. Labeling indicates the principal vibrating ions at $y=0$. For instance, ω_{Se1} is frequency of mode consisting mainly of Se vibrating against Cd in unit 1, etc. At other values of y, the S modes are very much mixed, as mentioned in text.

of CdSe for our model is given by[1]

$$\left[(k_1(1)+k_7-(4\pi/3+0.2)Ne^2_{\mathrm{Se},l})\Big/\left(\frac{M_{\mathrm{Cd}}M_{\mathrm{Se}}}{M_{\mathrm{Cd}}+M_{\mathrm{Se}}}\right)\right]^{1/2}. \tag{21}$$

An approximate relation between the short-range force constants and the compressibilities follows from the general relation given by Born and Huang[3]:

$$k_1(1)+k_7\approx\frac{3.2a_0\sqrt{3}}{B_{\mathrm{CdSe}}}, \tag{22}$$

where the lattice constant a_0 is listed in Table III. For hexagonal crystals, B is related to the elastic constants by the following expression[16]:

$$1/B=(2c_{11}+c_{33}+2c_{12}+4c_{31})/9. \tag{23}$$

[16] F. Seitz, *The Modern Theory of Solids* (McGraw-Hill Book Company, Inc., New York, 1940), p. 373.

The elastic constants for CdSe are given by Berlincourt *et al.*,[17] from which we calculated for the compressibility the value

$$B_{\mathrm{CdSe}}=1.88\times10^{-12}\ \mathrm{cm^2/dyn}.$$

This gives for $k_1(1)+k_7$ an appropriate value of 12.9×10^4 g/sec^2. Using the known TO frequency of CdSe for $\mathbf{E}\|$ (c axis) at 15°K (170 cm^{-1}), we solve for $e_{\mathrm{Se},l}$ from Eq. (21) and find $e_{\mathrm{Se},l}=8\times10^{-10}$ esu. The values finally chosen to give the best fit to the reflectivity curves for all values of y are $k_1(1)+k_7=11.26\times10^4$ g/sec^2, and $e_{\mathrm{Se},l}=6.5\times10^{-10}$ esu.

The compressibility of CdS, measured by Keyes,[18] is $B_{\mathrm{CdS}}=1.63\times10^{-12}$ cm^2/dyn. From this we obtain $k_2(5)+k_8=14.3\times10^4$ g/sec^2, and $e_{\mathrm{S},l}=8.4\times10^{-10}$ esu. The values finally chosen to give the best fit to the reflectivity curves are $k_2(5)+k_8=10.83\times10^4$ g/sec^2, and $e_{\mathrm{S},l}=5.5\times10^{-10}$ esu.

We emphasize that the expression for the compressibility in terms of nearest-neighbor force constants [Eq. (22)] is expected to be only approximate. Its value for our work lies therefore mainly in establishing starting values for the local charges and the two sets of nearest-neighbor force constants.

We notice that whereas the total charge of CdS is about 12% higher than that of GaP measured in I, the local charge of CdS is 5.5 times that of GaP. This is the reason why the frequency of the main mode of the S band increases as y increases rather than decreases, as is the case with the P band of the $GaAs_yP_{1-y}$ spectrum. The effect of the local charge on the frequency shift is even more pronounced in $CdSe_yS_{1-y}$, because the

TABLE IV. Classical oscillator parameters determined by curve fitting for $\mathbf{E}\|$ c-axis.

Nearest-neighbor force constants (g/sec^2)

Symbol	Cd-Se force constant	Cd-S force constant
$k_1(1)$	6.75×10^4	
$k_1(2)$	8.1×10^4	
$k_1(3)$	9.25×10^4	
$k_1(4)$	11.0×10^4	
$k_2(2)$		8.5×10^4
$k_2(3)$		8.1×10^4
$k_2(4)$		6.6×10^4
$k_2(5)$		6.8×10^4
k_7	4.5×10^4	
k_8		4.0×10^4

Next-nearest-neighbor force constants (g/sec^2)

Symbol	Between atoms	Force constant
k_3	Se-Se	-2.5×10^4
k_4	Se-S	1.0×10^4
k_5	S-S	2.25×10^4
k_6	Cd-Cd	0.5×10^4

Local effective ionic charges (esu)

$e_{\mathrm{Se},l}$	6.5×10^{-10}	$e_{\mathrm{S},l}$	5.5×10^{-10}

[17] D. Berlincourt, H. Jaffe, and L. R. Shiozawa, Phys. Rev. **129**, 1009 (1963).

[18] R. W. Keyes, J. Appl. Phys. **33**, 3371 (1962).

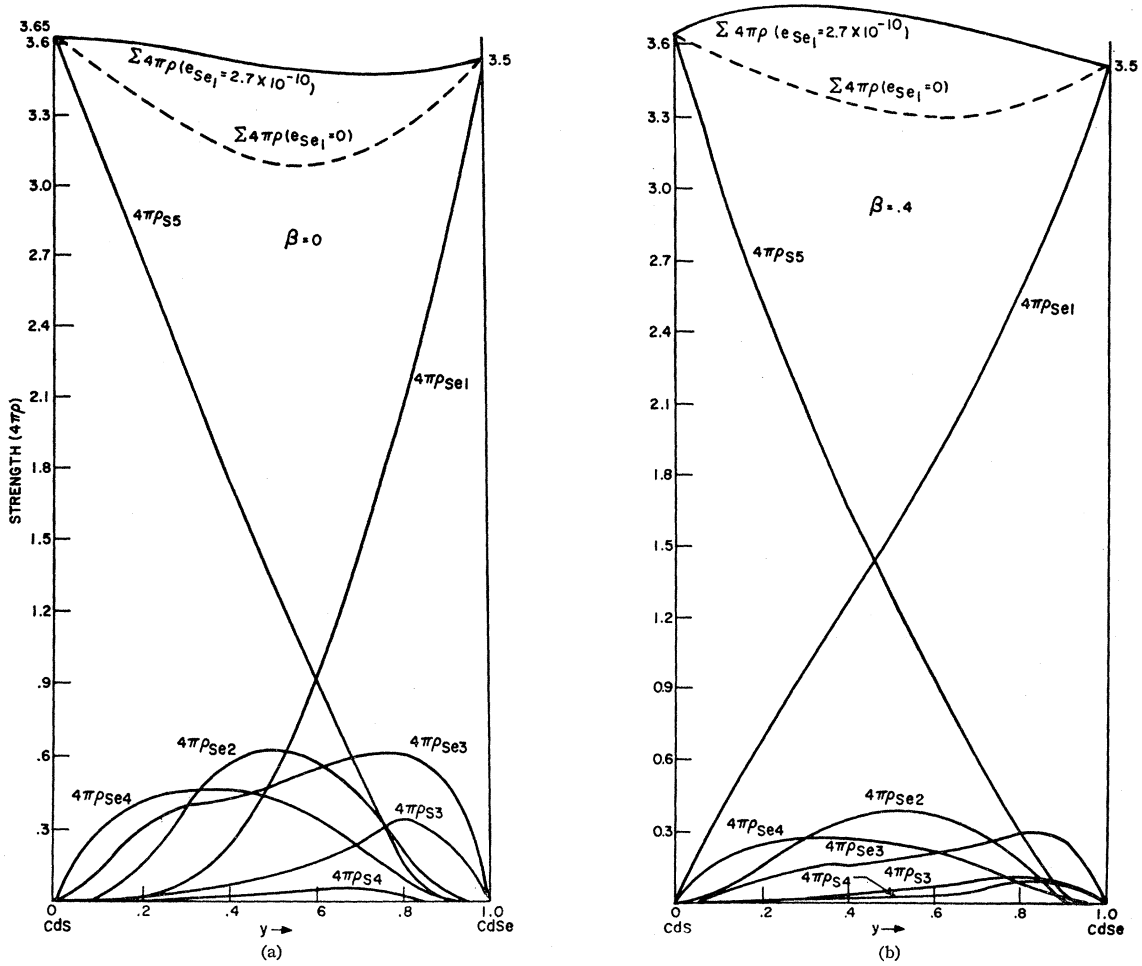

FIG. 17. Mode strengths versus composition (y), computed from the model. Labeling corresponds to Fig. 15. (a) $\beta=0$, (b) $\beta=0.4$.

short-range force constants are much smaller than in $GaAs_yP_{1-y}$.

After a few calculations of mode strengths with various sets of trial parameters, it was soon apparent that the total calculated strength of the Se modes was much below that of the experimentally required value, especially at low values of y. On the other hand, the total strength of the S modes was close to the required strength of the high-frequency band. Since the strength is directly proportional to the square of the effective ionic charge, it appears that the presence of sulphur in the lattice causes an increase in the ionicity of the Cd-Se bond. The following expression for the total effective ionic charge on a Se ion was found to give the correct strength of the Se band in the reflectivity spectra of $CdSe_ySi_{1-y}$:

$$e_{Se}=e_{Se,0}+(1-y)e_{Se,1}, \qquad (24)$$

where $e_{Se,0}$ is the effective ionic charge on Se in pure CdSe (11.15×10^{-10} esu). To obtain the correct strength of the Se band in the mixed crystals, we must take $e_{Se,1}=2.7\times10^{-10}$ esu. No such correction was found to be necessary for the effective ionic charge on the S ions. In Table IV, we have listed the set of force constants and charges which give a best fit to the reflectivity spectra of $CdSe_ySi_{1-y}$.

In Figs. 16 and 17, we have plotted the frequencies and strengths of the eight modes making up the two reststrahlen bands in the reflectivity spectra both for $\beta=0$ and $\beta=0.4$. As in the case of $GaAs_yP_{1-y}$, there are four additional optic modes, with low frequencies (around 100 cm^{-1}) and negligible strengths. An examination of the ion displacements of these four modes shows that they are primarily vibrations of entire neutral units against each other. In Figs. 17(a) and 17(b) we have drawn additional curves of the sum of the mode strengths obtained if no correction to the selenium charge is introduced [Eq. (24)]. The difference between this curve and the one including the correction is quite significant, showing the reason for the poor initial fits.

In Figs. 16 and 17, we have used labeling as in I for the normal modes. For example, S5 means that the eigenvector of this mode consists mostly of S ions

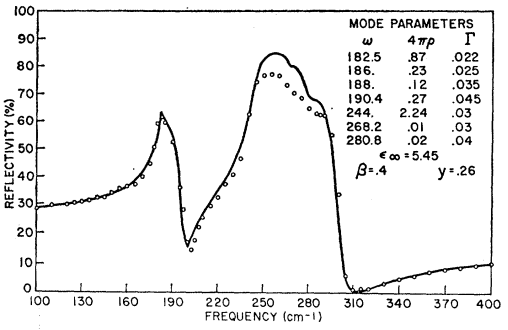

FIG. 18. Theoretical fit, based on model (solid line) of far-infrared reflectivity spectrum of $CdSe_{0.26}S_{0.74}$ at 15°K, with $\mathbf{E}\|$ (c axis). Open circles are experimental points.

vibrating against the Cd ion in unit 5. However, the S modes are considerably more mixed here than the Se modes. For example, the S5 mode consists of S moving against Cd in unit 5 near $y=0$, but consists of S moving against Cd in unit 4 near $y=1$. At intermediate values of y, the mode is mixed, i.e., it represents a vibration in which both the sulphur ions in units 4 and 5 vibrate against the Cd ions of these units.

In Figs. 18 to 20, we present the theoretical fit of the experimental reflectivity spectra for $y=0.26$, 0.53, and 0.75. The results for $y=0.985$ were presented in Fig. 9. The classical oscillator parameters and the value of β used in these fits are listed in the figures. The strengths of the various modes are exactly as calculated from the model. The frequencies are the calculated values $\pm\frac{1}{2}\%$; the damping constants were chosen to give a best fit and the high-frequency dielectric constants were obtained from

$$\epsilon_\infty(y)=y\epsilon_\infty(\mathrm{CdSe})+(1-y)\epsilon_\infty(\mathrm{CdS}). \qquad (25)$$

The value of the clustering parameter found to give the best fit was $\beta=0.4$ for all mixed crystals except the one with $y=0.985$, where $\beta=0$ gave better results. The degree of clustering of like negative ions in this crystal is thus only about one-half of that encountered in the $GaAs_yP_{1-y}$ system. We shall return to this matter in the next section.

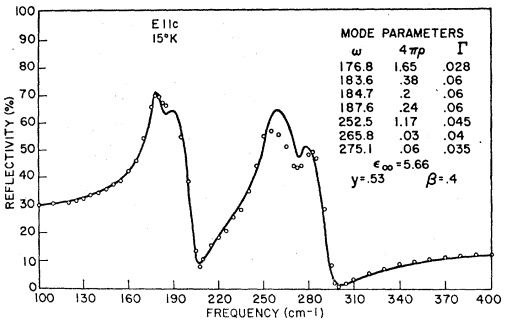

FIG. 19. Theoretical fit, based on model (solid line) of far-infrared reflectivity spectrum of $CdSe_{0.53}S_{0.47}$ at 15°K, with $\mathbf{E}\|$ (c axis). Open circles are experimental points.

In general, the theoretical reflectivity curves agree well with the measured reflectivity spectra except on top of the reststrahlen bands. This is not so much a question of mode strength or frequency, but of mode damping. Better fits could only be obtained by using frequency-dependent damping which causes greater damping near the mode center, but leaves the wings of the mode much the same as given by the values of damping constant chosen in our harmonic model.

To illustrate the importance of β, we have shown the reflectivity curve for $\beta=0$ when $y=0.75$ in Fig. 21. The same force constants and charges were used in the calculation of the strengths and frequencies listed in this figure as in Fig. 20. The damping constants were chosen to give a best possible fit. As can be seen, the results for $\beta=0$ are worse than for $\beta=0.4$ in several respects.

(1) The total strength of the S band is too large and that of the Se band is too small.

(2) There is a shift of strength from the main modes into the higher frequency modes in each band. This especially affects the fit in the S band.

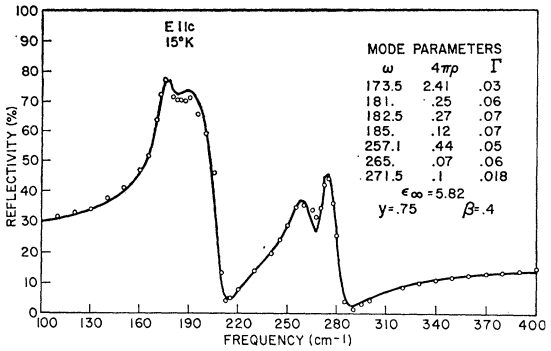

FIG. 20. Theoretical fit, based on model (solid line) of far-infrared reflectivity spectrum of $CdSe_{0.75}S_{0.25}$ at 15°K, with $\mathbf{E}\|$ (c axis). Open circles are experimental points.

(3) The frequencies of these last modes are incorrect as can be seen from the position of the dips in the theoretical curve.

Now, it is possible to remedy (1) if it is assumed that the Cd-Se bonds have become more ionic and the Cd-S bonds less, i.e., by further increasing the effective charge on Se and reducing the charge on S. It was found impossible, however, to change (2) and (3) without increasing β.

E. The Sulphur Local Mode

In I, a discussion was given of the impurity vibrations of very low concentrations of either As or P in $GaAs_yP_{1-y}$, where a local-mode approach is valid. Very little is known of the phonon density of states of CdS or CdSe, so no reliable local-mode calculations can be made. We can, however, make a rough estimate of the

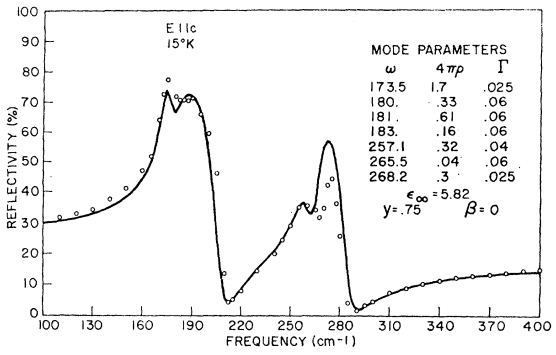

FIG. 21. Theoretical fit, based on model (solid line) of far-infrared reflectivity spectrum of $CdSe_{0.75}S_{0.25}$ at 15°K, with $\mathbf{E}\|(c$ axis). The force constants and charges used in the calculations are the same as for Fig. 19, but $\beta=0$, which results in a complete redistribution of strength between the modes. Open circles are experimental points.

local-mode frequency of S in CdSe. Since S is lighter than Cd or Se, it can produce a local mode at a frequency above the highest optical phonon of pure CdSe. Our approximation consists of assuming CdSe to have a phonon density of states like silicon (aside from frequency scaling) and taking Cd and Se to have equal mass. Using the methods of Dauber and Elliott[19] as in I, the mass-defect parameter is $\epsilon=0.66$, which predicts a local mode at $1.36\times\omega_{max}$. We identify ω_{max} with the highest-frequency infrared phonon which occurs at 210 cm^{-1}. The S local mode should then appear at 285 cm^{-1}. Experimentally we find this mode at 270 cm^{-1}, about 5% lower than the estimate (Figs. 9 and 10). For the case actually measured (1.5% S in CdSe), our model of the mixed crystal gives the correct S frequency since it takes into account mass and force-constant changes. The eigenvector given by the model shows that the S mode consists of Cd vibrating against S in unit 2 (i.e., isolated S). This is the behavior we expect for a local mode.

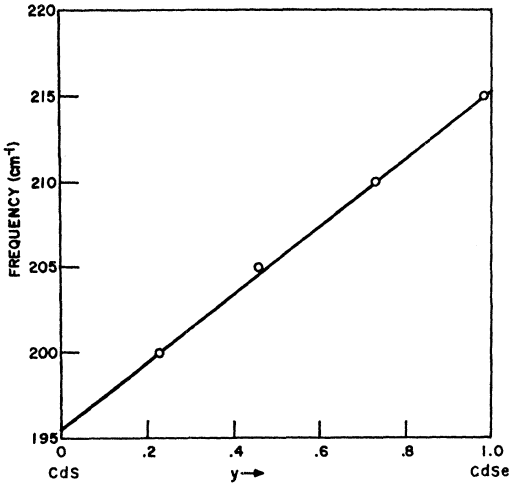

FIG. 22. Plot of minimum of low-frequency reflectivity band of $CdSe_ySi_{1-y}$ at 300°K. Model was not applied at this temperature, so curve is smooth line drawn through experimental points.

CONCLUSIONS

We have established that the model, which was originally developed to explain the significant features in the infrared reflectivity spectra of $GaAs_yP_{1-y}$, gives similar results for the alloy $CdSe_ySi_{1-y}$ at 15°K, by simply choosing a different set of force constants and charges. Although we established this result only for one polarization, we expect that a slightly different set of force constants and charges will yield an adequate fit for the other polarization.

The shift of the CdSe band with y can serve as a measure of the selenium content in a mixed crystal. The spectral feature easiest to observe is the reflectivity minimum of this band. In principle, we could have used the minimum of the high-frequency band (CdS) as well, but this is less well defined (see Figs. 11 to 13). Figure 22 shows the experimentally measured minima and the concentration as determined by the x-ray method. These are room-temperature data. The solid line, therefore, is not determined by the model, but is drawn to best fit the experimental points. It is interesting to note that the experimental points lie close to a straight line.

A significant result of this work is the nonzero value of the clustering parameter β, which had to be chosen to be 0.4. This value is much smaller than the value 0.75 required in the $GaAs_yP_{1-y}$ reflectivity fits.[1] For the $y=0.985$ sample, however, $\beta=0$ gives the best fit. For $GaAsiP_{1-y}$, a somewhat lower value of β was also observed at the end points of the concentration range.[1] Shockley has made calculations of the free energy for copper-gold alloys, based on nearest-neighbor bond energies and the entropy, which both depend on the state of order.[20] Both the existence of clusters ($\beta>0$), and the lower values of β found at the end points of the concentration range, appear to be consistent with Shockley's model, provided we assume that the Se-S bond energy is larger than the Se-Se and S-S bond energies and that the entropy is a maximum for $\beta=0$.

Note added in proof. Langer *et al.* (Phys. Rev. **152**, 788, 1966) have recently seen two longitudinal optic phonons in the edge emission of $CdSe_ySi_{1-y}$. Though their technique does not appear capable of resolving fine structure there is good agreement with the present work on the main LO mode frequencies at each concentration.

ACKNOWLEDGMENTS

The authors gratefully acknowledge valuable discussions with Professor H. G. Hartmann and assistance from J. A. Ditzenberger.

[19] P. G. Dawber and R. J. Elliott, Proc. Roy. Soc. (London) **A273**, 222 (1963); also Proc. Phys. Soc. (London) **81**, 459 (1963).

[20] W. Shockley, J. Chem. Phys. **6**, 130 (1938).